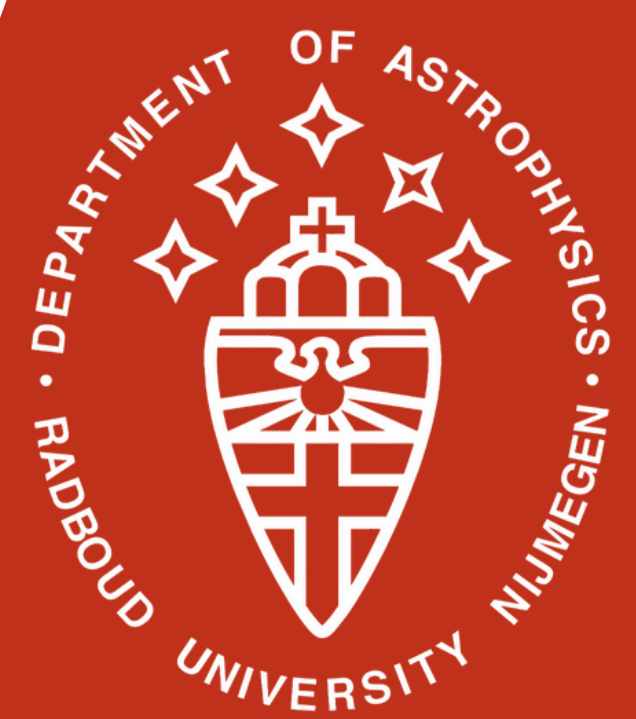


Radiative properties and multi-wavelength variability of two-temperature magnetically arrested disks

Maarten Wijdeveld*, Monika Mościbrodzka, Aristomenis Yfantis

Department of Astrophysics, Radboud University Nijmegen

*Email: maarten.wijdeveld@ru.nl



Overview

Magnetically arrested disks (MADs) are a subclass of radiatively inefficient black hole accretion disks where magnetic flux is accumulated on the horizon and undergoes cycles of rapid dissipation, which halts accretion and launches highly magnetised plasma outward. Such MAD models may be contenders for explaining the strong variability observed in both NIR and X-ray observations of Sagittarius A* (Sgr A*). As the thermodynamics of radiatively inefficient accretion flows are not well understood, we investigate MAD variability assuming a collisionless turbulent electron heating model and comparing this to a phenomenological parametrised disc-jet electron temperature prescription. We use Monte Carlo ray tracing [1] to construct spectral energy distributions (SEDs) and lightcurves from general relativistic magnetohydrodynamical (GRMHD) simulations of Sgr A* [3].

Electron Temperature Models

In our **turbulent heating** models [2], electron temperatures are self-consistently evolved alongside the GRMHD simulation [5] for both a non-spinning and highly spinning black hole [3]. The turbulent electron heating rate then strongly depends on

$$\beta = \frac{P_{\text{gas}}}{P_{\text{magnetic}}},$$

which is the ratio of gas to magnetic pressure.

Parametrised temperature models [4] directly 'paint on' the electron temperature based on the GRMHD proton temperature through

$$\frac{T_p}{T_e} = R_{\text{high}} \frac{1}{1+\beta^2} + R_{\text{low}} \frac{\beta^2}{1+\beta^2},$$

where R_{high} and R_{low} determine the respective coupling strength in the disk (high β ; $\beta \gg 1$) and along the jet wall (low β ; $\beta \ll 1$).

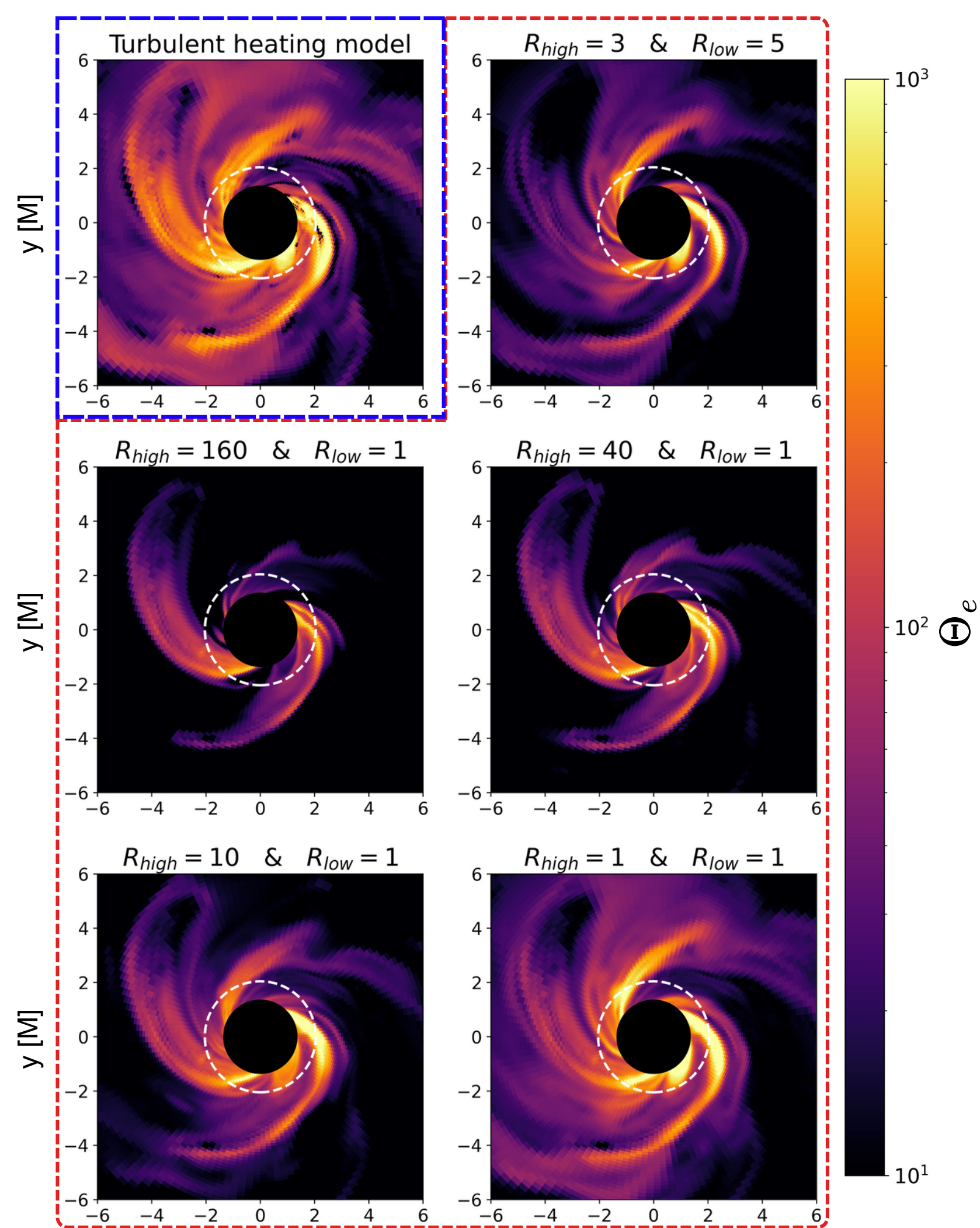


Fig. 1: Turbulent and parametrised dimensionless electron temperatures ($\Theta_e = k_B T_e / m_e c^2$) for a single time slice from our high spin ($a_* = 0.94$) simulation. The dashed white line represents the ISCO.

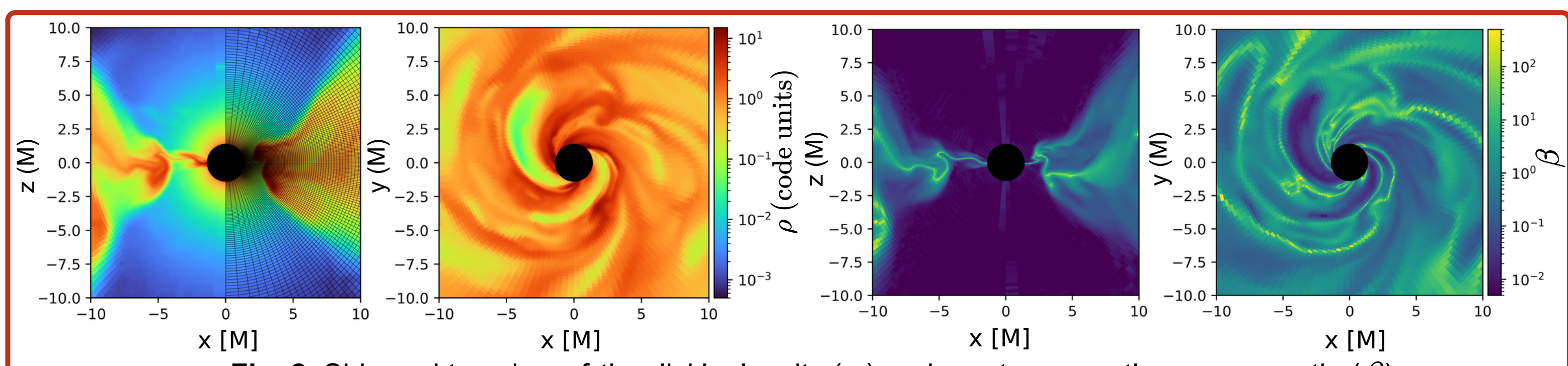
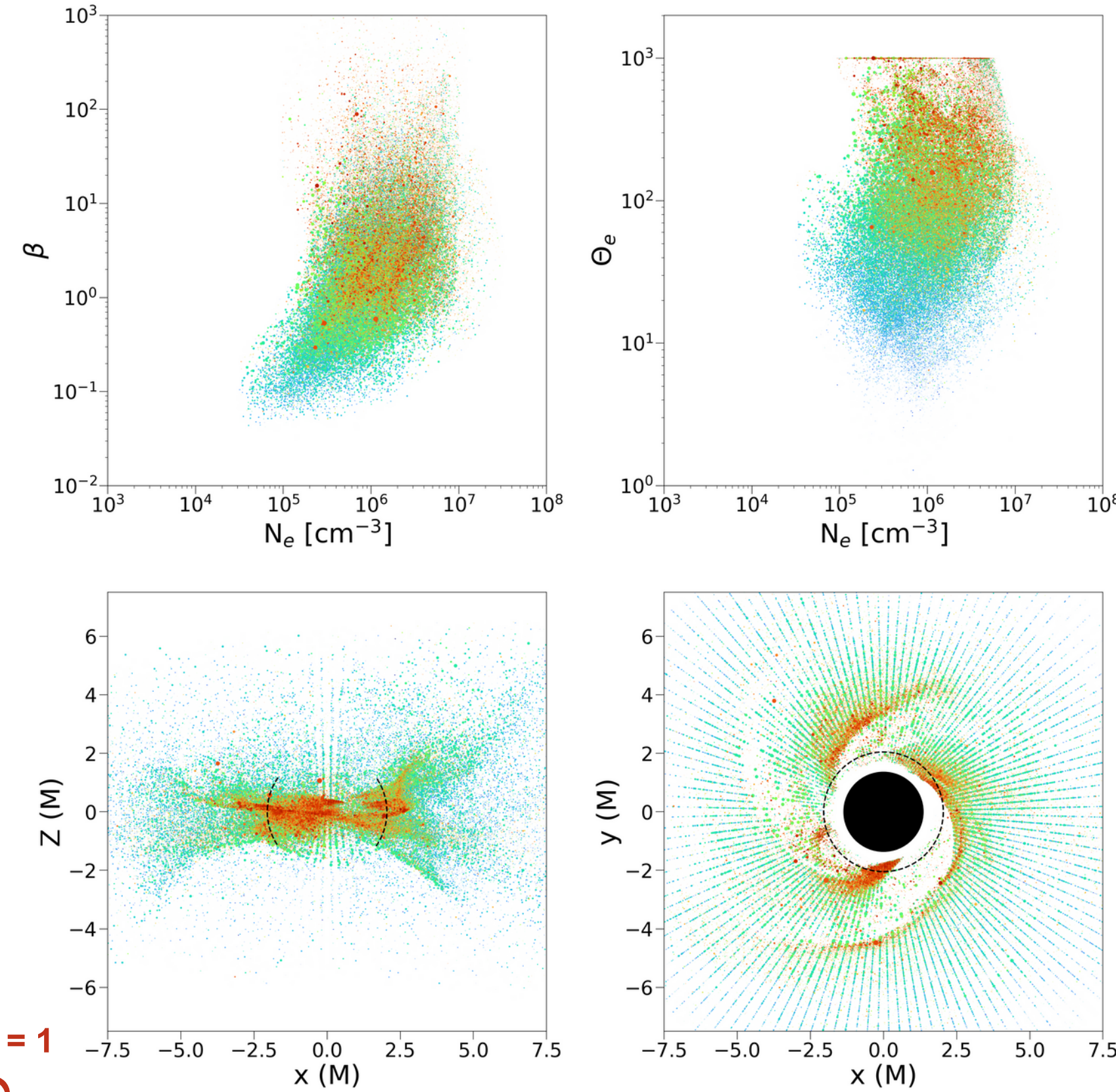


Fig. 2: Side and top view of the disk's density (ρ) and gas-to-magnetic pressure ratio (β)

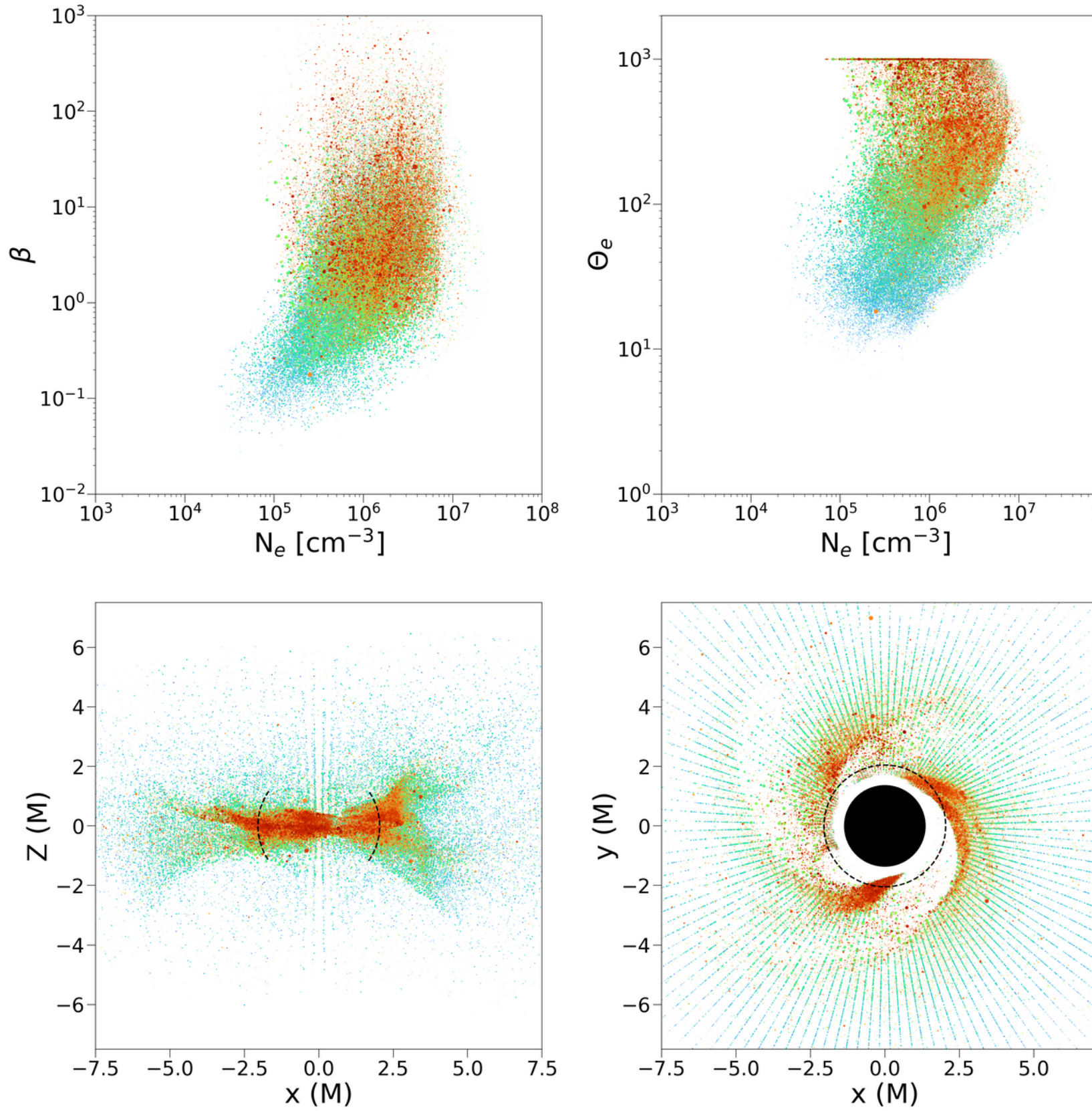
Ray-traced (Super)Photons: Origins and Plasma Properties

Turbulent heating



Movie of
 $R_{\text{high}} = 1 \text{ & } R_{\text{low}} = 1$

$R_{\text{high}} = 1 \text{ & } R_{\text{low}} = 1$



$R_{\text{high}} = 160 \text{ & } R_{\text{low}} = 1$

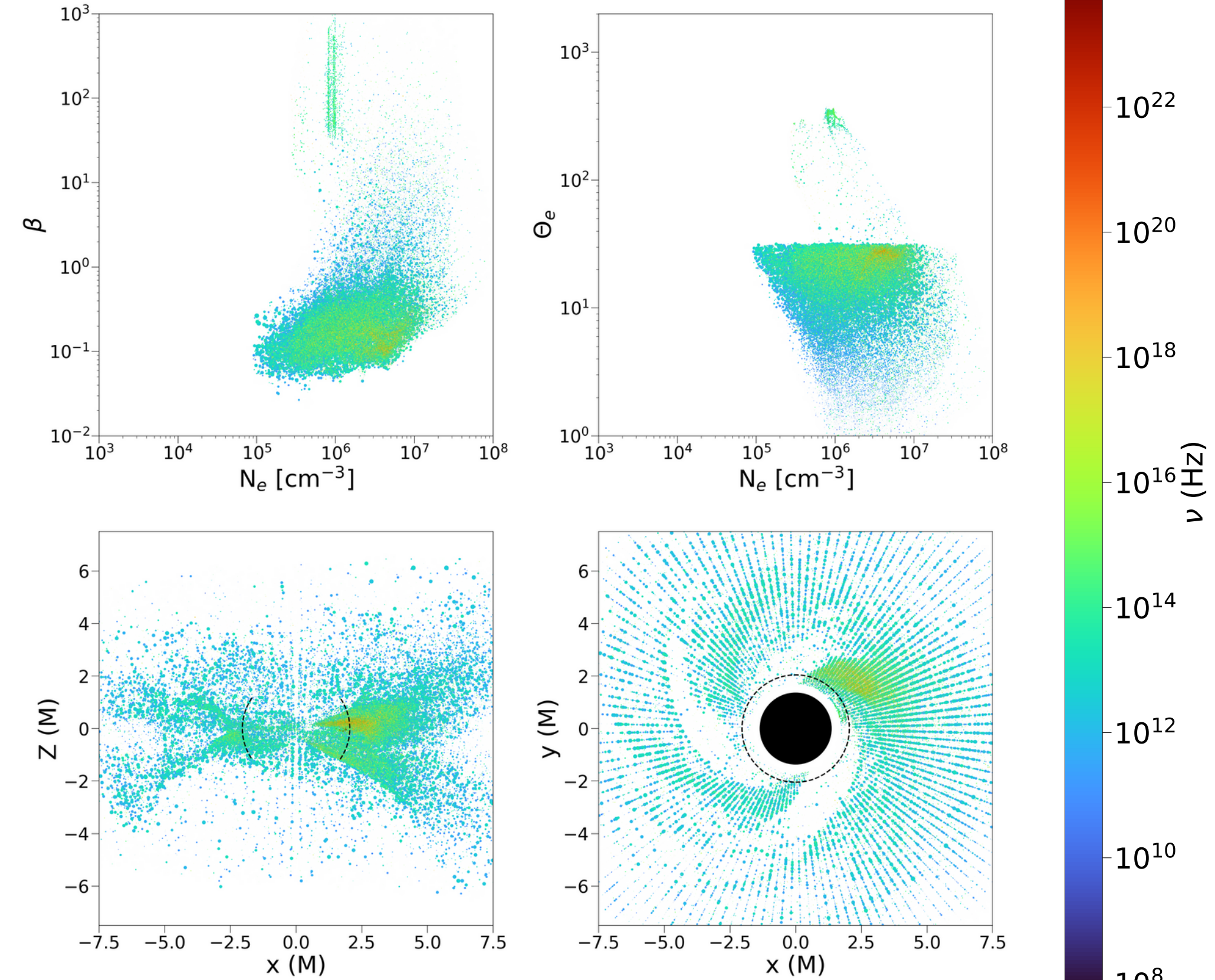


Fig. 3: Ray-traced superphoton origin during the same timeslice as depicted in Figs. 1 and 2. Both the turbulent heating and $R_{\text{high}} = 1 \text{ & } R_{\text{low}} = 1$ model result in emission originating from the inner parts of the dense spiral structures, where temperatures are highest ($\Theta_e = k_B T_e / m_e c^2$). Due to the high proton temperature in these regions β is large. The $R_{\text{high}} = 160 \text{ & } R_{\text{low}} = 1$ model is then too inhibited to reach similar electron temperatures there, resulting in, on average, much more extended emission from regions where $\beta \lesssim 1$. Note: We cut out emission from highly magnetised regions where our temperature models break down.

Spectral Energy Distributions

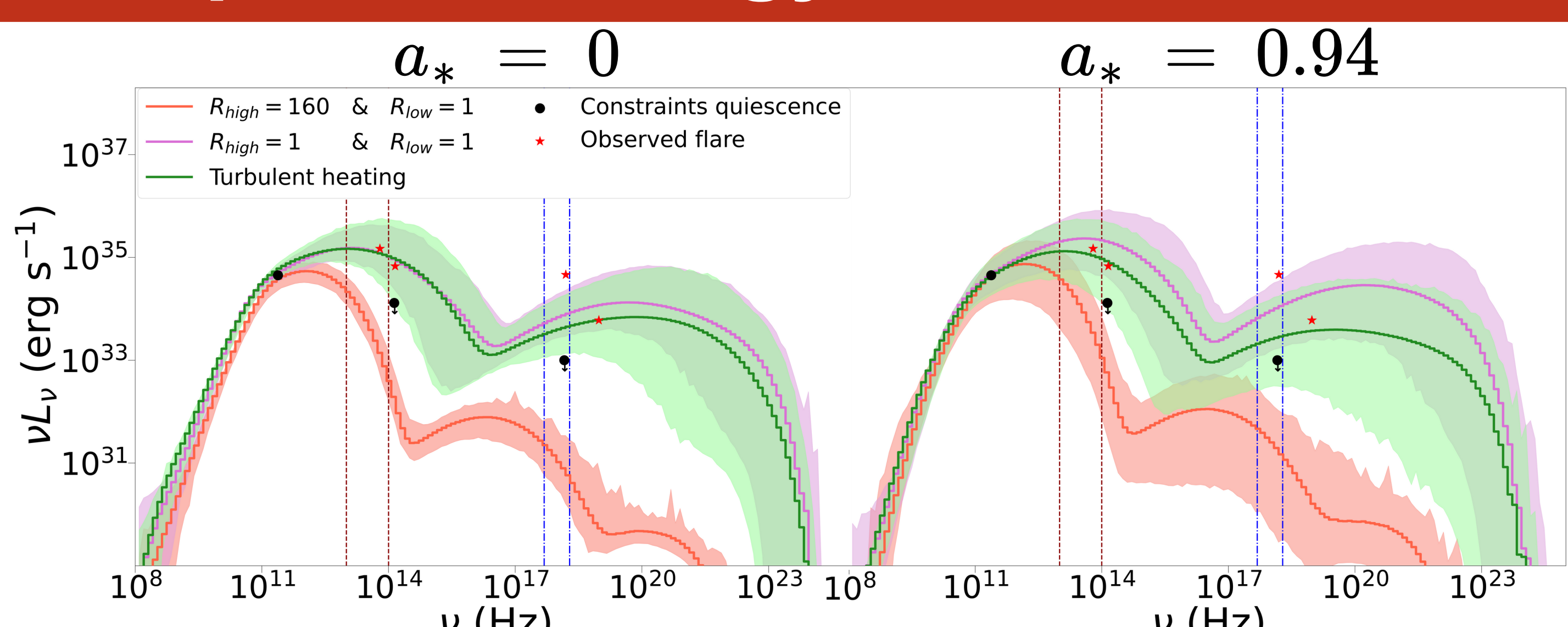


Fig. 4: Minimum to maximum spectral luminosity reached throughout ~28 hours of Sgr A* ray tracing (shaded regions) and the corresponding averages (solid lines). Here we show only results for our turbulent models (green) and our least luminous $R_{\text{high}} = 160$ (red) and most luminous $R_{\text{high}} = 1$ (purple) electron temperature parametrisations. Black dots correspond to quiescent constraints and red stars to observed NIR and X-ray flares [6][7]. Vertically red dashed and blue dash-dotted lines correspond to the frequency ranges used to calculate NIR (30-3 μm) and X-ray (2-8 keV) lightcurves in Fig. 5. Turbulent heating and $R_{\text{high}} = 1$ models overpredict quiescent constraints, but are able to match NIR and at least some X-ray flare luminosities. This is reversed for $R_{\text{high}} = 160$.

Near-IR and X-ray Lightcurves

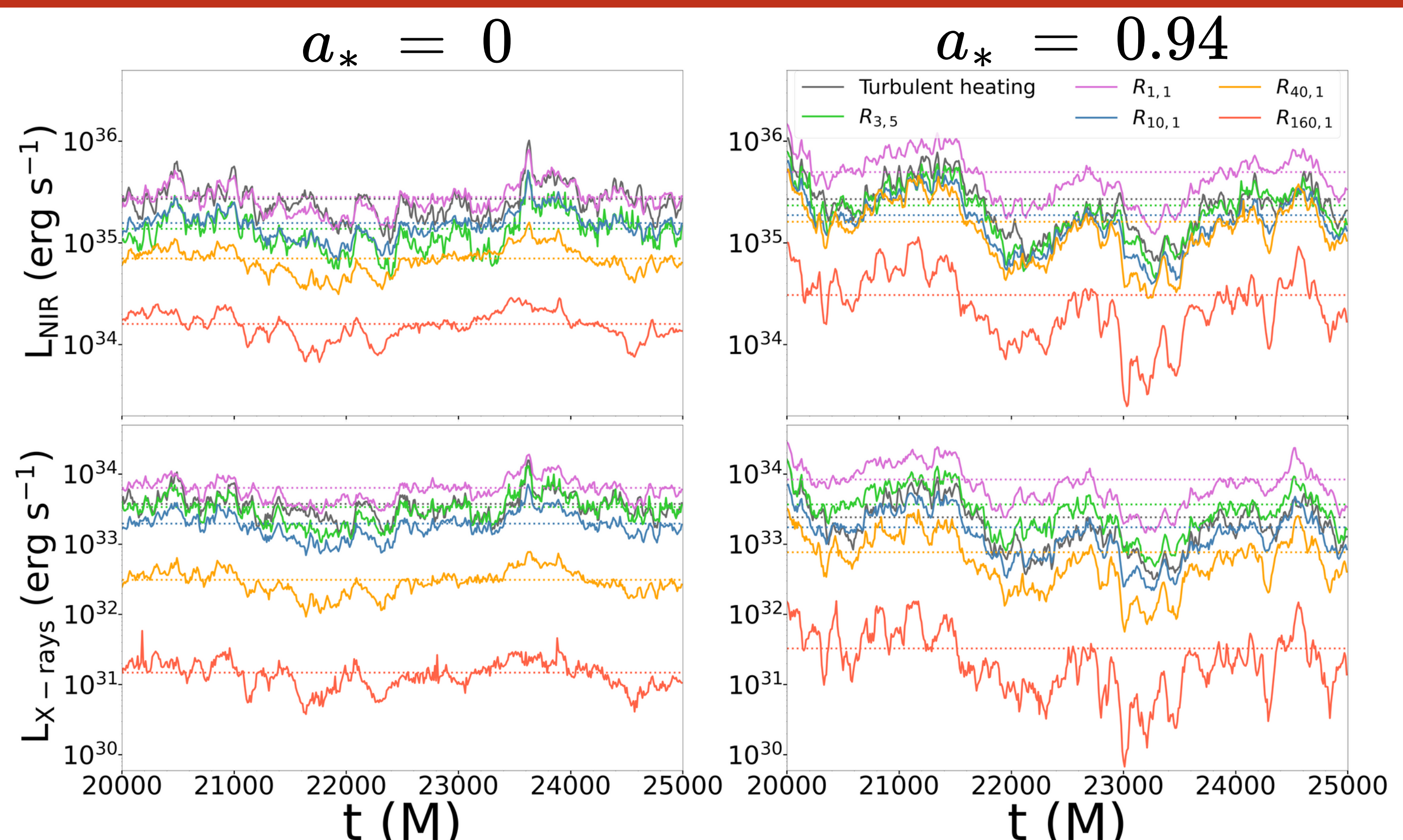


Fig. 5: Modelled NIR (30-3 μm) and X-ray (2-8 keV) lightcurves for all studied electron temperature models. e.g. $R_{3.5}$ denotes $R_{\text{high}} = 3 \text{ & } R_{\text{low}} = 5$. Only $R_{\text{high}} = 160$ high-spin models are capable of producing large luminosity variability ratios of $\gtrsim 10$ for NIR and $\gtrsim 100$ in X-rays. However, these are the result of drops in luminosity, rather than steep increases.

Conclusion

Turbulent and small- R_{high} -parametrised electron temperature models emit brightly from short-lived, compact, and hot regions in the disk. These models are capable of reaching observed flare luminosities, however, they overpredict quiescent emission and underpredict observed variability. In contrast, large R_{high} models stay within quiescent constraints, but generally exhibit more extended emission, not coupling well to the regions driving variability in hotter models.